15th Australasian Fluid Mechanics Conference
The University of Sydney, Sydney, Australia
13-17 December 2004

DNS of Turbulent Heat Transfer in a Channel Flow with a Streamwisely Varying Thermal Boundary Condition

Y. Seki[1] **and H. Kawamura**[1]

[1]Department of Mechanical Engineering,
Tokyo University of Science, 2641 Yamazaki Noda-shi, Chiba-ken, 278-8510, JAPAN

Abstract

Effect of thermal boundary condition is examined. The direct numerical simulation of turbulent heat transfer in a fully developed turbulent channel flow has been carried out for streamwisely varying thermal boundary conditions ($Re_\tau = 180$) with $Pr = 0.71$ to obtain the statistical mean temperature, the temperature variance, their budget terms and the time scale ratio etc. The obtained results have indicated that the time scale ratio varies along a stream direction.

Introduction

With the aid of recent developments in super and parallel computers, direct numerical simulation (DNS, hereafter) of turbulent flow is now often performed. The DNS is able to provide with a large amount of detailed data on the turbulent heat transfer with various thermal boundary conditions. Several experiments [4, 2] and turbulent modelling studies [7] for the streamwisely varying thermal boundary conditions had been carried out in the past studies. However, no DNS has been done for streamwisely varying thermal boundary conditions.

In the present study, effect of thermal boundary condition is examined. The DNS of turbulent heat transfer in a fully developed turbulent channel flow has been carried out for streamwisely varying thermal boundary conditions with $Pr = 0.71$, $Re_\tau = 180$, which is based on the friction velocity u_τ and channel half width δ, $Re_c = 6600$, which is based on the center velocity u_c and 2δ. The computational domains are given in figure 1. The computational domain is divided into three parts; the entrance region, the test region and the cooling (fringe) region. In the fringe region, an extra damping function is added in the energy equation to attenuate the temperature. Thus the periodic boundary condition can be applied in the streamwise direction with maintaining the inlet temperature to be zero.

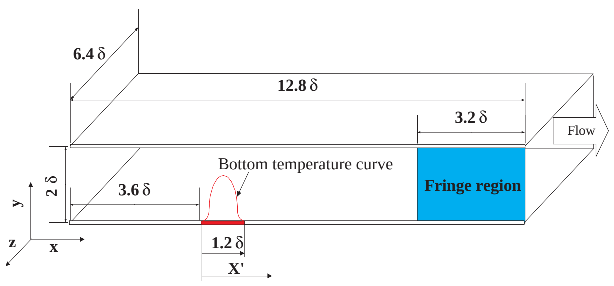

Figure 1: Configuration.

Numerical procedure

The DNS of turbulent heat transfer in a channel flow have been performed with Reynolds number of $Re_\tau = 180$ ($Re_c = 6600$) with $Pr = 0.71$. The computational domain is given in figure 1. Two infinite parallel plates are assumed. The buoyancy effect is not taken into consideration to examine the fundamental nature of the convective turbulent heat transfer in this research.

The coordinates and flow variables are normalized by the channel half width δ, the kinematic viscosity ν, the friction velocity u_τ, and the maximum temperature of the bottom wall T_{max}. The fundamental equations are the continuity equation:

$$\frac{\partial u_i^+}{\partial x_i^*} = 0, \tag{1}$$

and the Navier-Stokes equation:

$$\frac{\partial u_i^+}{\partial t^*} + u_j^+ \frac{\partial u_i^+}{\partial x_j^*} = -\frac{\partial p^+}{\partial x_i^*} + \frac{1}{Re_\tau}\frac{\partial^2 u_i^+}{\partial x_j^{*2}} + \frac{\partial \bar{p}^+}{\partial x_1^*}\delta_{i1}. \tag{2}$$

Here, $i = 1$, 2 and 3 indicate the streamwise, wall-normal and spanwise directions, respectively. The variables t and p are the time and the pressure. The superscript $*$ indicates that the variables are normalized by δ. The third term in the right-hand side of Eq. (2) is the streamwise mean pressure gradient. The boundary condition for the momentum field is

$$u_i^+ = 0, \qquad \text{at } y = 0 \text{ and } 2\,\delta. \tag{3}$$

The enegy equation for the instantaneous temperature $T^+(x^*, y^*, z^*)$ is expressed as

$$\frac{\partial T^*}{\partial t^*} + u_j^+ \frac{\partial T^*}{\partial x_j^*} = \frac{1}{Re_\tau \cdot Pr}\frac{\partial^2 T^*}{\partial x_j^{*2}} - Q(x). \tag{4}$$

The endothermal term ($Q(x) = \lambda(x)T^*$) is non-zero only in the fringe (cooling) region, where fringe function $\lambda(x)$ is the strength of the cooling with a maximum of inverse number of the time step Δt^{*-1}. The form of $\lambda(x)$ is designed to minimize the upstream temperature influence. The heating condition at the bottom wall is

$$\begin{gathered} T_{wall}(\xi) = T_{\max}(\sin \pi\xi)^2 \\ if\ 0 \le \xi \le 1,\ \ else\ T_{wall}(\xi) = 0 \ \ \text{at } y = 0, \\ where\ \ \xi = x - x_o,\ \ x_o = 3D_L = 3.6\delta. \end{gathered} \tag{5}$$

where D_L is the heated streamwise length of 1.2δ. Figure 2 shows the thermal boundary condition given by equation (5) at the bottom wall. On the other hand, the thermal boundary condition at the top wall is assigned to be zero.

$L_x \times L_y \times L_z$	$N_x \times N_y \times N_z$	Δx^+	Δy^+	Δz^+
12.8δ×2δ×6.4δ	512×128×256	4.5	0.2～5.9	4.5

Table 1: Computational conditions.

The simulation has been made with the use of the finite difference method in which special attention is paid to the consistency between the analytical and numerical differential operations [5]. The method was confirmed to give good agreement with the spectral method [6]. The present numerical scheme consistent with the analytical operation ensures the balance of the transport equations for the statistical correlations such as the temperature variance and the turbulent heat flux. A fourth-order central difference scheme is adopted in the streamwise and spanwise directions, and the second-order central difference scheme is used in the wall-normal direction. Further details of the method can be found in [1], [5] and [6]. The computational condition is shown in table 1. The computation has been performed with the use of 8 processing elements of VPP5000 at Kyushu University.

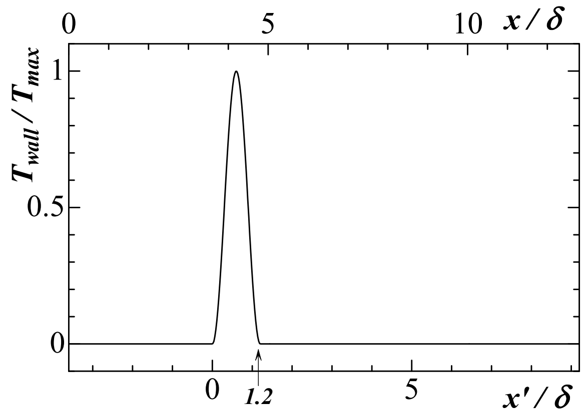

Figure 2: Variation of bottom wall temperature.

Results and discussion

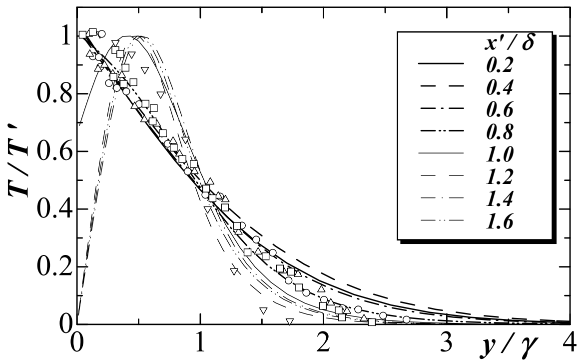

Figure 3: Mean temperature, symbols are experimental data [9], $\bigtriangledown$:$x' = 9.6$, $\triangle$:$x' = 37.2$, $\bigcirc$:$x' = 75.6$, $\square$:$x' = 122.4$.

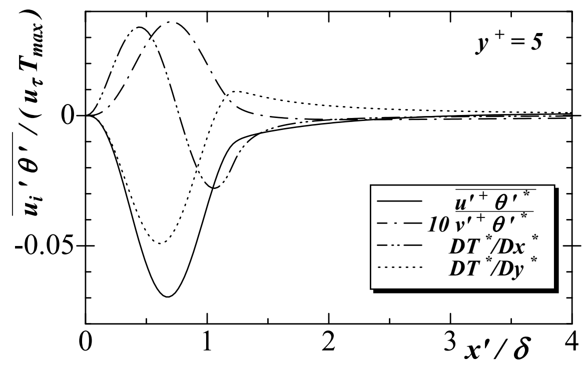

Figure 4: Turbulent heat flux.

Mean temperature profiles are shown in figure 3. If the maximum temperature (above ambient) T' and the normal distance γ from the wall where $T = 0.5T'$ occurs are chosen as the temperature and length scales respectively, the values of DNS (upstream of $x'/\delta = 0.8$) are similar to experimental data [9] of heated wall-Cylinder immersed in a turbulent boundary layer.

Figure 4 shows the turbulent heat flux $\overline{u'\theta'}$ and $\overline{v'\theta'}$ in the near wall region. The interesting feature of figure 4 is that the counter gradient diffusion exists for $\overline{u'\theta'}$ behind $x'/\delta = 0.8$. The counter gradient diffusion is observed behind $x'/\delta = 1.1$ for $\overline{v'\theta'}$ as well.

Turbulent Prandtl number

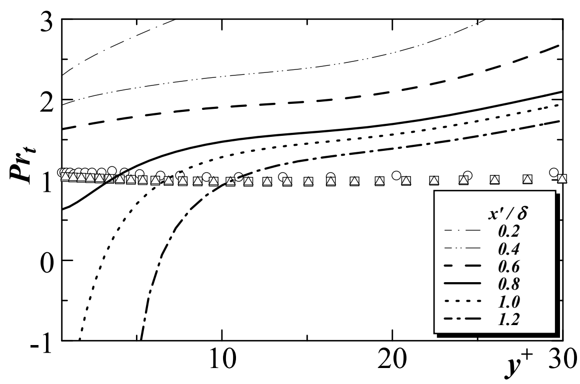

Figure 5: Turbulent Prandtl number, $\bigcirc$:Uniform heat source [3], $\triangle$:Constant wall temperature difference [8], $\square$:Uniform heat flux heating [8].

The turbulent Prandtl number Pr_t, defined as the ratio;

$$Pr_t \equiv \frac{\overline{u^+v^+}}{\overline{v^+\theta^*}} \frac{d\bar{T}^*/dy^+}{d\bar{u}^+/dy^+} \tag{6}$$

of momentum diffusivity to thermal diffusivity, has been evaluated from the present data at several stations and is shown in figure 5. The calculated results [3] for uniform heat source is plotted in figure 5. The other calculated results of the constant wall temperature difference and the uniform heat flux heating by authors' group [8] are also plotted in figure 5. In most of the existing studies, Pr_t tends to be the constant value of 1.0 for several thermal boundary conditions [3, 8]. In the case of the present streamwisely varying thermal boundary condition, however, figure 5 shows that Pr_t is totally different than the constant value of 1.0. This tendency is qualitatively similar to that reported in [2]. Generally, Pr_t is used to obtain the turbulent heat flux from the mean temperature gradient. Figure 5, however, indicates that it cannot be used for the estimation of the turbulent heat flux in case of the thermal boundary condition with rapid streamwise variation, because it changes significantly along the streamwise direction.

Time scale ratio

The time scale ratio R is expressed as the ratio of the scalar time scale $\tau_\theta (= k_\theta/\varepsilon_\theta)$ to the momentum one $\tau_u (= k/\varepsilon)$;

$$R = \frac{\tau_\theta}{\tau_u} = \frac{k_\theta}{\varepsilon_\theta}\frac{\varepsilon}{k}. \tag{7}$$

Because the velocity field is the fully developed turbulent channel flow in this study, the momentum time scale $\tau_u (= k/\varepsilon)$ is constant along the streamwise direction. Therefore, the scalar time scale $\tau_\theta (= k_\theta/\varepsilon_\theta)$ determines R along the streamwise direction. Figure 6 shows the distribution of the time scale ratio. The wall-asymptotic value of R is analytically equal to the molecular Prandtl number. The near-wall limiting value of R

given in figure 6 becomes indeed the molecular Prandtl number irrespective of the streamwise direction. On the other hand, the obtained result in figure 6 has indicated that the time scale ratio varies along the streamwise direction in the outer region.

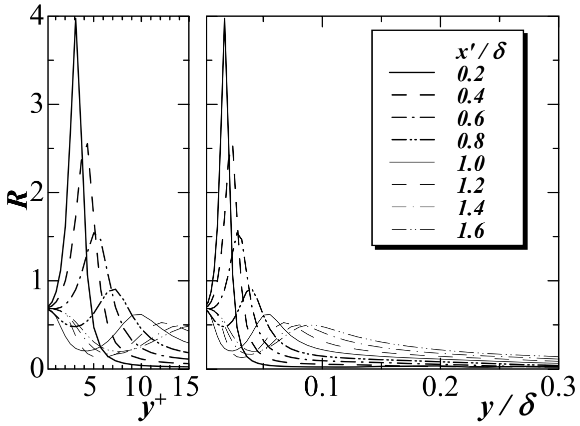

Figure 6: Time scale ratio.

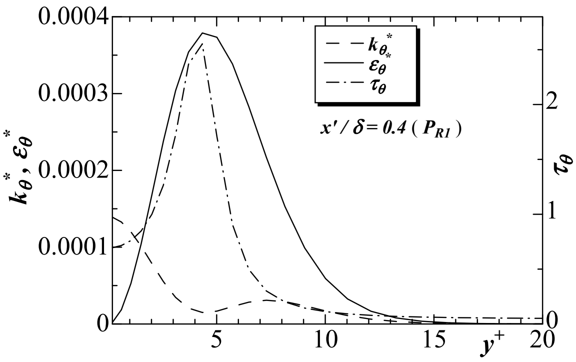

Figure 7: k_θ^* and its dissipation rate.

The value of R at the position $x'/\delta = 0.4$ is significantly higher than the unity at $y^+ = 4.3$ in figure 6. As can be seen from figure 7, it results from the value of the temperature variance k_θ in excess of those of other height at $y^+ = 4.3$. Moreover, the local minimal value of its dissipation rate ε_θ is also observed at $y^+ = 4.3$ in figure 7. The local maximal value around $y^+ = 0, 7.5$ occurs to dissipate the energy transported from the portion of large energy by the molecular and turbulent diffusion. In fact, the local minimal value of the dissipation rate necessarily exists at the peak of the temperature variance. Therefore, the peak of the time scale ratio surely occurs at $y^+ = 4.3$.

R is shown in figure 8 where a abscissa axis is assigned to the streamwise direction. It indicates that the time scale ratio varies along the streamwise direction. To examine the peak of both P_{R1} and P_{R2}, the budget for k_θ^* is shown in Fig. 9. The positions where the maximal and minimal peaks of the time scale ratio exist are in agreement with those of the production term for k_θ^*. In the case of the present streamwisely varying thermal boundary condition, the specific feature of P_{k_θ} is that the negative value of P_{k_θ} exists in latter half of the heated section. To explain the negative value of the production term P_{k_θ}, the terms which constitute P_{k_θ} in the transport equation of k_θ^* are examined. It is given by

$$P_{k_\theta} = -\overline{u'\theta'}\frac{d\overline{T}}{dx} - \overline{v'\theta'}\frac{d\overline{T}}{dy}. \qquad (8)$$

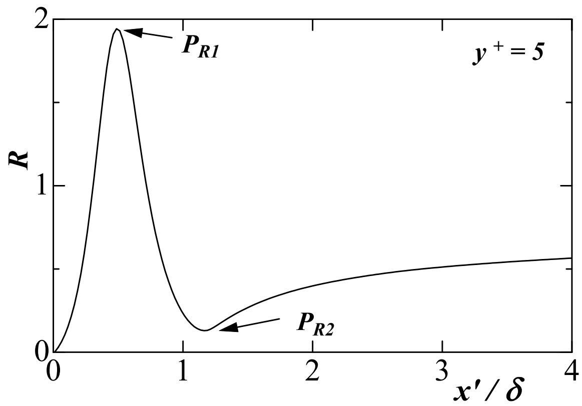

Figure 8: Time scale ratio at the inner region.

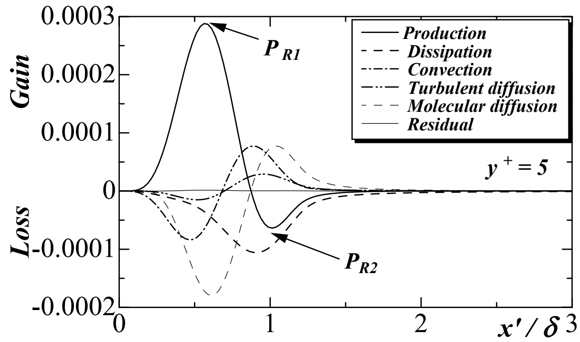

Figure 9: Budget of k_θ^*.

The relation among $\overline{u'\theta'}$, $d\overline{T}/dx$, $\overline{v'\theta'}$, $d\overline{T}/dy$ is seen in figure 4. In the position of the negative value of P_{k_θ}, $\overline{u'\theta'}$ and $d\overline{T}/dx$ stay negative value. Moreover, other constitutive terms stay positive value in the region.

Figure 10 shows the two dimensional distribution for the production term P_{k_θ} of the k_θ^*. Solid line shows the positive value and Dashed line shows the negative value, respectively. The negative region of the production term occupies a fairly large area behind the heated section. This is because the hot convection is transported from the upstream, and thus the mean temperature gradient is inverted in the near-wall region. The two dimensional distribution of R is also shown in figure 11. The specific feature of R is that the local maximum exists in the heated section and the local minimum in latter half of the heated section. A noticeable agreement in the profiles of P_{k_θ} and R is observed through the comparison of figures 10 and 11. The region of the negative of P_{k_θ} is in good agreement with that of the local minimum of R.

Figure 12 indicates that the tendency of the balance between k_θ and ε_θ is the same at any downstream position. It is also shown that the peaks of both k_θ and ε_θ are transported to the central region of the channel along the streamwise direction. One can notice that, in general, ε_θ is high where k_θ is large. More detailed inspection indicates that the contour of ε_θ possesses a large number of inflection points than that of k_θ. We have seen in figure 8 that the position of the local minimum in ε_θ corresponds to the maximum point of k_θ. This trend can be observed also in the two-dimensional contour of ε_θ, which causes the more complex profile of ε_θ than that of k_θ.

Conclusions

The DNS of turbulent heat transfer in a fully developed turbulent channel flow has been carried out for streamwisely varying thermal boundary conditions with $Pr = 0.71$, $Re_\tau = 180$ ($Re_c = 6600$). The thermal turbulence statistics such as the mean temperature, temperature variance, its dissipation terms, turbulent Prandtl number, time scale ratio have been discussed.

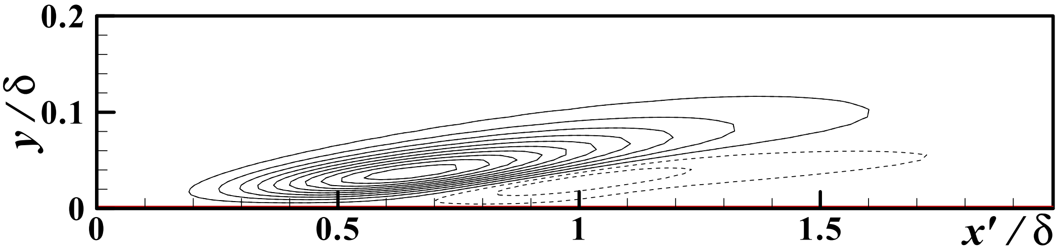

Figure 10: Side views of the production term for k_θ^*. Solid line are the positive value and dashed line are the negative one. Contour level is from -1.0×10^{-4} to 3.0×10^{-4} with increments of 5.0×10^{-5}.

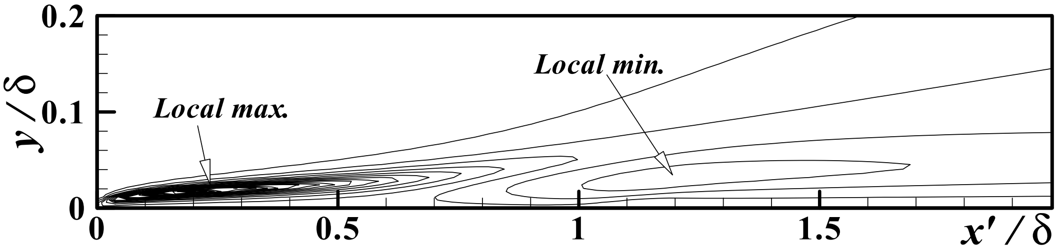

Figure 11: Side views of the time scale ratio R. Contour level is from 0.2 to 4 with increments of 0.2.

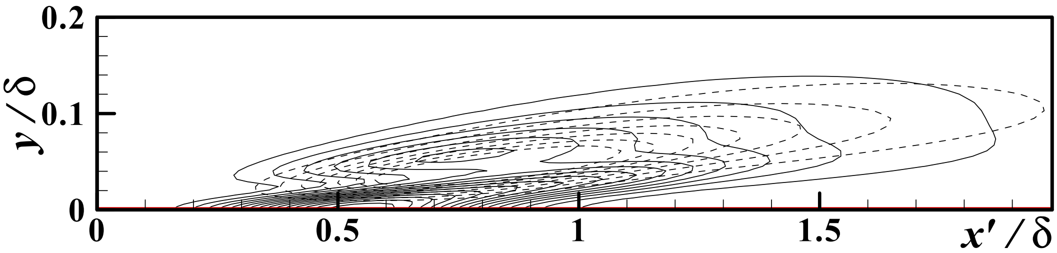

Figure 12: Side views of k_θ^* (dot line) and ε_θ^* (solid line). Contour level for k_θ^* is from 1.7×10^{-4} to 8.7×10^{-4} with increments of 1.0×10^{-4}, while that of ε_θ^* is from 1.1×10^{-6} to 1.7×10^{-4} with increments of 1.0×10^{-5}.

In this present study, the presented turbulent Prandtl number cannot be used for estimating because it changes rapidly with x due to the rapid variation in the thermal boundary condition. The time scale ratio also varies along the streamwise direction in the outer region. It results from the tendency that the value of k_θ tends to become rapidly smaller than that of ε_θ in the near-wall region behind the heated section. Moreover, it has been confirmed that the local minimal value of ε_θ necessarily exists at the peak of the temperature variance.

Acknowledgements

This calculations were performed with the use of the VPP-5000 at Kyushu University.

References

[1] Abe, H., Kawamura, H. and Matsuo, Y., Direct numerical simulation of a fully developed turbulent channel flow with respect to Reynolds number dependence, *ASME J. Fluids Eng.*, **123**, 2001, 382–393.

[2] Antonia, R.A., Danh, H.Q. and Prabhu, A., Response of a Turbulent Boundary Layer to a Step Change in Surface Heat Flux, *J. Fluid Mech.*, **80**, 1977, 153–177.

[3] Antonia, R.A. & Kim, J., Reynolds shear stress and heat flux calculations in a fully developed turbulent duct flow, *Int. J. Heat Mass Transfer*, **34**, No. 8, 1991, 2013–2018.

[4] Johnson, D.S., Velocity and Temperature Fluctuation Measurements in a Turbulent Boundary Layer Downstream of a Stepwise Discontinuity in Wall Temperature, *J. Appl. Mech., Trans. A.S.M.E.*, **26**, 1959, 325–336.

[5] Kawamura, H., Direct numerical simulation of turbulence by finite difference scheme, *In: Zhang, Z. S.* & *Miyake, Y. (Eds.), The Recent Developments in Turbulence Research*, International Academic Publishers, 1994, 54–60.

[6] Kawamura, H. and Kondoh, Y., Application of consistent finite difference scheme to DNS of turbulent heat transfer in channel flow, *Proc. 3rd KSME/JSME Therm. Eng. Conf., Kyongju, Korea*, **1**, 1996, 53–58.

[7] Nagano, Y., Hattori, H. and Abe, K., Modeling the Turbulent Heat and Momentum Transfer in Complex Flows under Various Thermal Conditions, *Proc. of Int. Symp. on Math. Modelling of Turbulent Flows, Tokyo, Japan*, 1995, 79–86.

[8] Seki, Y., Abe, H. and Kawamura, H., DNS of turbulent heat transfer in a channel flow with different thermal boundary conditions, *Proc. 6th ASME/JSME Therm. Eng. Conf., USA*, 2003, 248.

[9] Sreenivasan, K.R., Danh, H.Q. and Antonia, R.A., Diffusion form a heated wall-cylinder immersed in a turbulent boundary layer, *Proc. of Thermaofluids Conf., Hobart*, 1976, 103–106.